Carrier-Mediated Transport through Bulk Liquid Membranes: Dependence of Transport Rates and Selectivity on Carrier Properties in a Diffusion-Limited Process[1]

Jean-Paul Behr,* Michèle Kirch,* and Jean-Marie Lehn*

Contribution from the Institut Le Bel, Université Louis Pasteur, 4, rue Blaise Pascal,[2] 67000 Strasbourg, France. *Received June 14, 1984*

Abstract: A diffusion-limited kinetic treatment has been applied (i) to carrier-mediated transport of a single substrate species and of an ion pair and (ii) to carrier-mediated exchange diffusion of two substrates against a back-transported species. Extensive numerical simulation has been performed in order to describe the relation of transport rates and selectivities with thermodynamic properties (extraction equilibria) of the carrier–substrate pairs. Transport rates display a bell-shaped dependence on equilibrium extraction constants; they decrease when there is either too little substrate extraction at the entry or too much extraction at the exit of the membrane set-up; the domain over which transport is optimal depends on the particular process involved and on the experimental conditions employed. The determination of transport selectivities of a given carrier between different substrates requires direct competition experiments, transport selectivities being close to thermodynamic extraction selectivities only when there is little complex formation at the exit interface. This treatment has been applied to a number of literature results on transport through liquid membranes, involving widely different substrates, carriers, and experimental conditions; it is found that the diffusion-limited process accounts in a straightforward fashion for the experimental data and that there is no need to invoke a mechanism where transport is limited by complexation kinetics.

The development during the last 15 years of selective receptor molecules for cationic as well as anionic, organic, or inorganic substrates led to their use as carrier agents for inducing selective transport through artificial or biological membranes. Thus, a chemistry of transport processes has built up, promoted by the design of synthetic carrier molecules and actively pursued in numerous laboratories (for an overview of recent aspects, see ref 3). Much attention has been given to carriers for metal cations. In view of the great variety of their structures, they display a broad range of binding features and of cation exchange rates, ranging from fast exchange in the complexes of acyclic ligands to very slow exchange in the most stable macropolycyclic cryptates. As a consequence, transport rates markedly depend on the nature of the carrier, in a given set of conditions. In addition to their chemical interest and their relevance to biological transport, three-phase transport processes, where the carrier operates selective and catalytic translocation, have also many advantages over two-phase extraction and are being widely employed in separation science involving bulk liquid, supported, or emulsion membranes.

Most of the work performed with synthetic carriers has made use of such thick membranes. Our own studies have been concerned with various transport processes,[4] going in particular from amino acid transport by acyclic carriers[5] to cation transport by cryptands and other macrocyclic ligands.[6-8] In order to better understand the relationship between carrier properties and transport rates, it became desirable to adapt and extend earlier kinetic treatments to the investigation of the effects produced by specific physicochemical parameters characterizing the carriers and the complexes which they form. The extensive work reported in recent years on transport and carriers in liquid membrane systems raised the need for stating *explicitly* in specific cases the consequences implicitly contained in the general equations developed earlier. The approaches to the mathematical description of carrier transport with different rate-limiting assumptions are derived from the work of Rosenberg and Wilbrandt,[9] Jacquez,[10] or Blumenthal and Katchalsky.[11] Although these models behave alike for a low saturation of the carrier, this is not the case with regard to the requirements for a simultaneously efficient (high mass transfer) *and* selective transport process. Thus knowledge of the step, i.e., either membrane diffusion or interfacial reaction, which limits the rate of transport is of much importance for the setup of further experiments and the design of carrier molecules.[4] We have resumed Wilbrandt's hypotheses on a membrane diffusion limiting step to describe simply and quantitatively various transport mechanisms. This model, and the one derived assuming an interfacial reaction-limiting step, will be discussed further in the light of the available literature data on the facilitated transport of various inorganic and organic ions.

Facilitated Diffusion of a Single Substrate Species. The simplest process is schematically depicted in Figure 1: a substrate S is taken up from the aqueous *in* phase by complex formation with a membrane-soluble ligand L, the complex diffuses across the membrane, S is subsequently released into the aqueous *out* phase, and the regenerated free carrier diffuses back. The driving force of the transport is the concentration difference between the aqueous phases. Usually L and LS are partitioned essentially in favor of the membrane whereas the reverse holds for S. As long as the rates for complex formation and dissociation are fast compared to diffusion through the membrane (see below), the L and LS concentrations at the membrane interfaces (i), and the corresponding S aqueous concentrations are related through the overall extraction equilibrium constant K_e:

$$K_e = \frac{LS_{i,in}}{L_{i,in}S_{i,in}} = \frac{LS_{i,out}}{L_{i,out}S_{i,out}} \quad (1)$$

When all phases are stirred, concentrations may be considered constant throughout the bulk of each phase and concentration gradients are restricted to the unstirred boundaries[12] (Nernst layers

(1) Presented in part at the Third Symposium on Macrocyclic Compounds, Provo, Utah, August 1979.
(2) ERA No. 265 of the Centre National de la Recherche Scientifique.
(3) Spach, G., Ed. "Physical Chemistry of Transmembrane Ion Motions"; Elsevier: Amsterdam, 1983.
(4) Lehn, J. M. *Pure Appl. Chem.* **1979**, *51*, 987-995. Lehn, J. M. pp 181-207 in ref 3.
(5) Behr, J. P.; Lehn, J. M. *J. Am. Chem. Soc.* **1973**, *95*, 6108-6110.
(6) (a) Kirch, M.; Lehn, J. M. *Angew. Chem., Int. Ed., Engl.* **1975**, *14*, 555-556. (b) Kirch, M. Thèse de Doctorat-ès-Sciences, Université Louis Pasteur, Strasbourg, 1980.
(7) Bacon, E.; Jung, L.; Lehn, J. M. *J. Chem. Res.* **1980**, 1967-1987.
(8) Hriciga, A.; Lehn, J. M. *Proc. Natl. Acad. Sci. U.S.A.* **1983**, *80*, 6426-6428.
(9) Rosenberg, T.; Wilbrandt, W. *Exp. Cell Res.* **1955**, *9*, 49-67; *Pharmacol. Rev.* **1961**, *13*, 109-183.
(10) Jacquez, J. A. *Biochim. Biophys. Acta* **1964**, *79*, 318-328.
(11) Blumenthal, R.; Katchalsky, A. *Biochim. Biophys. Acta* **1969**, *173*, 357-369.

0002-7863/85/1507-0241$01.50/0

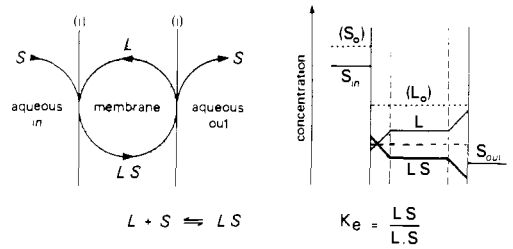

Figure 1. Left: Schematic representation of the carrier (L) mediated transport of a subtrate S. Right: Typical concentration profile in the steady state.

at the interfaces). Let us assume as a first approximation that the concentrations $S_{i,in}$ and $S_{i,out}$ at the interfaces are equal to the concentrations S_{in} and S_{out}, respectively, in the bulk aqueous phases; the transport rate is then limited by diffusion through the organic unstirred layers. If the thickness (l) and areas of both layers are the same, and since the diffusion coefficients D_L and D_{LS} are usually similar, Fick's first law under steady-state conditions imposes all concentration gradients to be equal. Therefore the ligand and complex concentration profiles are symmetric with respect to $L_0/2$ (Figure 1).

$$LS_{i,in} - LS = LS - LS_{i,out} = L - L_{i,in} = L_{i,out} - L$$

$$\text{thus, } LS = (LS_{i,in} + LS_{i,out})/2 \qquad (2)$$

The rate of transport V, expressed in moles per unit time per unit surface, may then be written as

$$V = \frac{D}{l}(LS_{i,in} - LS) = \frac{D}{2l}(LS_{i,in} - LS_{i,out})$$

These interfacial quantities are related to the aqueous substrate concentrations through (eq 1) and since the total ligand concentration L_0 is constant throughout the membrane ($L_0 = LS_{i,in} + L_{i,in} = L + LS = LS_{i,out} + L_{i,out}$),

$$LS_{i,in(out)} = K_e L_0 \frac{S_{in(out)}}{1 + K_e S_{in(out)}}$$

The rate equation then becomes

$$V = \frac{D}{l}\frac{L_0}{2}K_e\frac{S_{in} - S_{out}}{(1 + K_e S_{in})(1 + K_e S_{out})} \qquad (3)$$

which is first order with respect to the carrier concentration L_0. Following eq 1, $K_e S_{in(out)}$ is the carrier loading ($LS_{in(out)}/L_{in(out)}$) at the interfaces. Depending on the experimental conditions, three regimes may be observed: at low saturation of the carrier at both interfaces ($K_e S_{in(out)} \ll 1$), the rate is low and first order with respect to the substrate concentration; as more complex is formed at the *in* interface (higher substrate concentration or higher extraction constant), the rate increases as

$$V \sim \frac{D}{l}\frac{L_0}{2}K_e\frac{S_{in} - S_{out}}{1 + K_e S_{in}}$$

up to its maximum

$$V_{max} = (D/l)(L_0/2) \qquad (4)$$

which is independent of $S_{in(out)}$ and K_e; at this stage of the saturation kinetics, the carrier is *half-filled* by the substrate ($LS = L = L_0/2$) and the interfacial concentrations of carrier and complex (Figure 2a) are $LS_{i,in} \sim L_{i,out} \sim L_0$, $LS_{i,out} \sim L_{i,in} \sim 0$, giving the largest concentration gradient; when complex formation at the *out* interface can no longer be neglected,[13] an increase in the second term of the denominator in (3) decreases the rate of transport, and for a high saturation at both interfaces ($K_e S_{in(out)} \gg 1$) one has $V \propto K_e^{-1}$ and $LS \sim L_0$ (Figure 2b), i.e., the carrier is filled by **S** and almost no transport is observed.

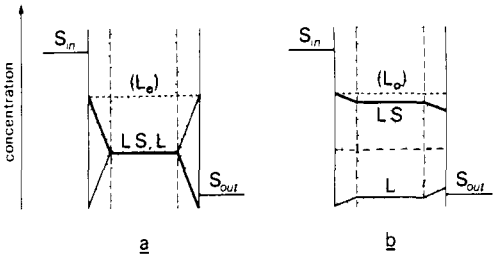

Figure 2. Concentration profiles in the cases of (a) high saturation of the carrier at the *in* interface and (b) high saturation at both interfaces.

Thus, the rate of transport of a substrate does not follow uniformly its affinity for the carrier nor its concentration, a fact more documented than expounded in the literature (although shown both experimentally[14] and theoretically[9] by Wilbrandt some 20 years ago !).

The approximation made above, of neglecting the gradients in the aqueous unstirred layers, is valid if $S_{in(out)} > L_0$. At the beginning of an experiment, this is usually not the case for S_{out} which has to be smaller than $S_{i,out}$ in order to fulfill the steady-state condition $V = (D/l)(S_{i,out} - S_{out})$; extracting the diffusion resistance from eq 4 yields

$$S_{i,out} = S_{out} + \frac{L_0}{2}\frac{V}{V_{max}} \qquad (5)$$

It is convenient to express the *out* concentration at a given time as a fraction f of the initial concentration S_0 in the *in* phase; if the amount of substrate in the organic phase can be neglected, and if the volumes of the aqueous phases are identical

$$S_{out} = fS_0 \qquad (0 \leq f \leq \tfrac{1}{2})$$

$$S_{in} = (1 - f)S_0 \qquad (6)$$

The relevant rate equation is similar to (3) except that $S_{i,out}$ replaces now S_{out}. Replacement of variables by their expressions (5) and (6) yields

$$\frac{V}{V_{max}} = K_e\frac{S_0(1 - 2f) - (L_0/2)(V/V_{max})}{[1 + K_e S_0(1 - f)][1 + K_e S_0 f + (K_e L_0/2)(V/V_{max})]} \qquad (7)$$

This equation has been computed (Appendix A) as $V/V_{max} = g(\log K_e)$ for a given set of total concentrations (S_0, L_0) at various stages (f) of an experiment (Figure 3). It yields bell-shaped curves which are superimposed at their left-edge and behave as a saturable process *as long as complex formation at the out interface is negligible*, leading to a very flat maximum for low f values. A given experiment (S_0, L_0, K_e fixed, f variable) being a vertical section through the bundle of curves, the rate of transport remains relatively constant only for $K_e \ll |K_e|_{max}$. For higher values of the extraction constant, V decreases rapidly with f so that *measuring an "initial rate" is not founded anymore.* For $f \to 0$, $|K_e|_{max}$ varies like $(S_0 L_0)^{-1/2}$ and the width of the curves depends on (S_0/L_0).

Facilitated Diffusion of an Ion Pair. This is the system most widely studied,[15-18] especially in relation to the transport of bound monovalent cations (C^+) together with an external anion (A^-), by neutral ligands (L) like crown ethers and cryptands (see Figure 4).

With the same hypotheses as previously, and setting the initial concentrations $C^+ = A^- = S_0$, the rate equation corresponding to (3) is

$$V = V_{max}K_e\frac{S_{in}^2 - S_{out}^2}{(1 + K_e S_{in}^2)(1 + K_e S_{out}^2)} \qquad (8)$$

(12) (a) Shean, G. M.; Sollner, K. *Ann. N.Y. Acad. Sci.* **1966**, *137*, 759-776. (b) Sollner, K. In "Diffusion Processes, Proceedings of the Thomas Graham Memorial Symposium, University of Strathclyde"; Scherwood, J. N., Chadwick, A. V., Muir, W. M., Swinton, F. L. Eds.; Gordon and Breach: London 1971; Vol. 2, pp 655-730.

(13) By principle, $S_{i,out}$ (and here S_{out}) cannot be set equal to zero, since this would be in contradiction with the basic assumption of thermodynamic equilibrium, eq 1.

(14) Wilbrandt, W. *J. Cell Comp. Physiol.* **1956**, *47*, 137-145.

(15) Reusch, C. F.; Cussler, E. L. *AIChE J.* **1973**, *19*, 736-741.

(16) Wong, K. H.; Yagi, K.; Smid, J. *J. Membr. Biol.* **1974**, *18*, 379-397.

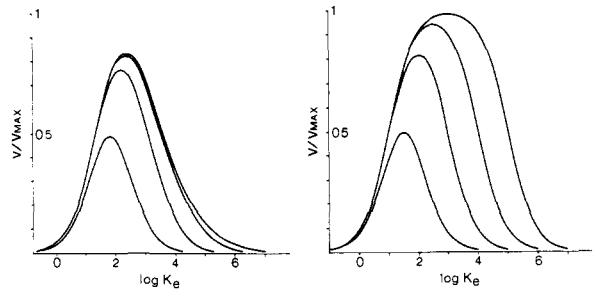

Figure 3. Variation of the rate of carrier mediated transport of a substrate (Figure 1, left) as a function of the thermodynamic extraction equilibrium constant K_e. The rate is expressed as the ratio V/V_{max}, where V_{max} is the maximum rate given by eq 4. In addition to its dependency on the initial concentrations of ligand (L_0) and substrate (S_0) (left diagram: $L_0 = 10^{-3}$ M; $S_0 = 5 \times 10^{-2}$ M; right diagram: $L_0 = 10^{-6}$ M; $S_0 = 10^{-1}$ M) the shape of a particular curve is also a function of the extent of transport at the time where the rate is determined; each family of curves corresponds to a fraction $f = 0.01$, 0.1, 1, and 10% of substrate transported on going from the highest to the lowest curve.

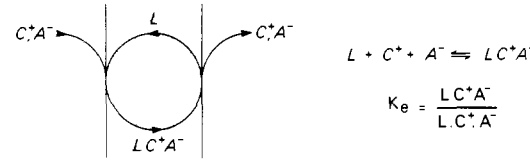

$$L + C^+ + A^- \rightleftharpoons LC^+A^-$$

$$K_e = \frac{LC^+A^-}{L.C^+.A^-}$$

Figure 4. Schematic representation of the carrier (L) mediated transport of an ion pair (C^+,A^-).

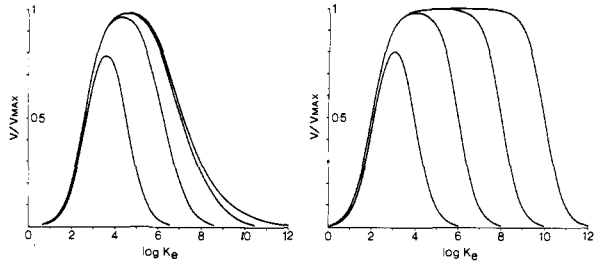

Figure 5. Graph of the rate of facilitated diffusion of an ion pair (Figure 4) vs. the thermodynamic extraction equilibrium constant K_e; the parameters corresponding to the different curves are the same as in Figure 3.

Computation with the more realistic condition in eq 5 (see Appendix B) yields the curves shown in Figure 5. The overall shape of V/V_{max} vs. log K_e is similar to that of the transport of a single substrate species, and the same conclusions are valid here (see above). Due to the simultaneous extraction and transport of two species (C^+ and A^-), concentrations appear at the second power in the rate equation and therefore $|K_e|_{max}$ varies here like $(S_0L_0)^{-1}$ for $f \rightarrow 0$ and the width of the curves like $(S_0/L_0)^2$. Thus, the range of K_e where transport occurs depends on the concentrations. Since usually 5×10^{-2} M $< S_0 < 5 \times 10^{-1}$ M and 10^{-3}M $< L_0 < 5 \times 10^{-3}$ M, transport is calculated to be *most efficient for* log $|K_e|_{max} \sim$ 4–6 (see also Figure 5), as has been found experimentally.[6,17]

Exchange Diffusion of Two Substrates. When the carrier bears a net charge, it has to transport back a counterion S_2 which is exchanged against the forward transported S_1, as shown in Figure 6. The equilibrium constant K_e is dimensionless and represents the relative affinity of the substrates S_1 and S_2 for L.

With the usual approximations and initial concentrations $S_{1,in} = S_{2,out} = S_0$, a trivial treatment gives

$$V = V_{max}K_eS_0\frac{S_{in} - S_{out}}{(S_{in} + K_eS_{out})(S_{out} + K_eS_{in})} \qquad (9)$$

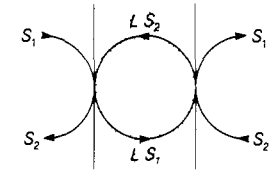

$$LS_1 + S_2 \rightleftharpoons LS_2 + S_1$$

$$K_e = \frac{LS_1.S_2}{LS_2.S_1}$$

Figure 6. Schematic representation of the facilitated exchange diffusion of two substrates S_1 and S_2.

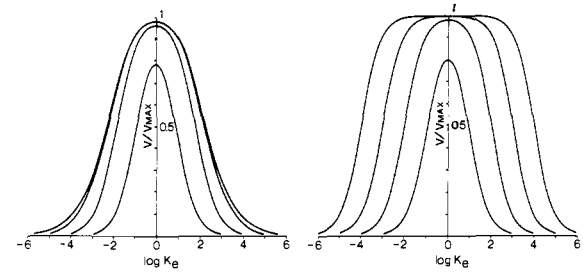

Figure 7. Graph of the rate of facilitated exchange diffusion of two substrates (Figure 6) vs. the thermodynamic extraction equilibrium constant K_e; the parameters corresponding to the different curves are the same as in Figure 3.

As for the rate eq 3 and 8, the straightforward proportionality between V and K_e is divided by the product of the carrier saturations at the interfaces.

The graphical representation (see Appendix C) in Figure 7 shows a major difference with respect to the previous ones (Figures 3 and 5): the bundle of curves is *symmetrical* with respect to log $K_e = 0$. This is a consequence of the symmetrical character of the exchange process (Figure 6) which allows also simple calculations to be performed (Appendix C): derivation shows that the transport rate is maximum (whatever S_0, L_0, f) for $K_e = 1$, i.e., when the two substrates have the *same affinity for the carrier* (as shown experimentally[19]); the fastest rate attainable is

$$|V/V_{max}|_{max} = (1 - 2f)(1 - (L_0/S_0))$$

i.e., the rate of diffusion at half saturation (eq 4) of the carrier in the membrane ($V_{max} = (D/l)(L_0/2)$) diminished by the extent of total transport ($2f$) and by the ratio of total carrier over substrate concentrations (L_0/S_0); the range of extraction constant where transport is efficient, as measured by the width at half-height of the curves in Figure 7 for $V = V_{max}/2$, is

$$\Delta(\log K_e)_{1/2} \sim 2 \log \frac{1 - 2f}{f + (L_0/4S_0)}$$

which varies again as $(S_0/L_0)^2$ for $f \rightarrow 0$.

Substrate Competition. Transport Selectivity. The goal of most transport experiments through bulk liquid membranes (and also emulsion membranes which obey the same rules) is to achieve the selective removal of a given substrate among others. The thermodynamic extraction selectivity K_{eA}/K_{eB} of a ligand for two substrates S_A and S_B is in no case directly related to the relative rates of transport V_A, V_B measured in *separate* experiments. As shown in the previous sections, *all* following situations can occur, depending on the experimental conditions

$$\text{with } K_{eB} \ll K_{eA} \ll |Ke|_{max}: \qquad V_B < V_A$$

$$\text{with } K_{eB} \ll |K_e|_{max} \ll K_{eA}: \qquad V_B \lesssim V_A \text{ or } V_B \gtrsim V_A$$

$$\text{with } K_e|_{max} \ll K_{eB} \ll K_{eA}: \qquad V_B > V_A$$

Transport selectivity between S_A and S_B should only be measured in true competition experiments. Furthermore, above $|K_e|_{max}$ the

(17) Lamb, J. D.; Christensen, J. J.; Oscarson, J. L.; Nielsen, B. L.; Asay, B. W.; Izatt, R. M. *J. Am. Chem. Soc.* **1980**, *102*, 6820–6824.

(18) Burgard, M.; Jurdy, L.; Park, H. S.; Heimburger, R. *Nouv. J. Chim.* **1983**, *7*, 575–578.

(19) Lehn, J. M.; Moradpour, A.; Behr, J. P. *J. Am. Chem. Soc.* **1975**, *97*, 2532–2534.

Table I. Literature Data on Transport Experiments through Stirred Bulk Liquid Membranes and Calculated V_{max}^{rep}/L_0 Values (V_{max}^{rep} is, Among Many Substrates, the Maximum Reported Rate of Transport; L_0 is the Total Carrier Concentration)

substrate	carrier	membrane: solvent, area of interfaces (cm^2)	highest reported rate: V_{max}^{rep} [a]	L_0 (M)	V_{max}^{rep}/L_0 [b]	ref
phenylalaninate	methyltricaprylylammonium (aliquat 336)	toluol, 14	5×10^{-3}	1×10^{-2}	0.5	5
Rb^+P^- [c]	beauvericin	$CHCl_3$, 0.8	3.5×10^{-5}	6.5×10^{-5}	1.8 [d]	21
Na^+P^-	4′-methylbenzo-18-crown-6	$CHCl_3$, 1.43	2.9×10^{-4}	2×10^{-3}	4.2 [d]	16
C_6H_5-CH(OH)-CO_2^-	(−)-*N*-(1-naphthyl)methyl-α-methylbenzylammonium	$CHCl_3$, 2	1.6×10^{-1}	1.2×10^{-1}	2.9 [d]	19
K^+P^-	dibenzo-18-crown-6	$CHCl_3$, 13	5.7×10^{-4}	7×10^{-4}	0.8	22
phenethylammonium chloride	dicyclohexyl-18-crown-6	$CHCl_3$, 2.5	6.4×10^{-2}	5×10^{-2}	1.3	7
Li^+P^-	hexapyrazolic macrocycle	$CHCl_3$, 6.15	5.7×10^{-4}	7×10^{-4}	0.8	23
K^+P^-	dibenzo-18-crown-6	$CHCl_3$, 2.5	1.5×10^{-3}	1.5×10^{-3}	1 [e]	6b
Li^+P^-	cryptand[2.2.1]	$CHCl_3$, 2.5	1.5×10^{-3}	1.5×10^{-3}	1 [e]	6b
K^+	lipophilic tartro-18-crown-6 monocarboxylate	$CHCl_3$, 1.54	1.1×10^{-3}	5.5×10^{-4}	2	24
o-$O_2NC_6H_4CO_2^-$	lipophilic copper(II) complex	CH_2Cl_2, 9.5	3×10^{-3}	5×10^{-3}	0.6	25
K^+	lipophilic diazatetraoxa-18-crown-6 monocarboxylate	$CHCl_3$, 5	2×10^{-3}	1×10^{-3}	2	26
Cs^+	*p-tert*-butylcalix[8]arene	CH_2Cl_2/CCl_4 (25/75)	3.6×10^{-3}	1×10^{-3}	3.6	27
$Ag^+NO_3^-$	dicyclohexyl-18-crown-6	$CHCl_3$	3.7×10^{-3}	1×10^{-3}	3.7	28
$Na^+NO_3^-$	cryptand[2.2.2$_B$]	$CHCl_3$	5×10^{-3}	1×10^{-3}	5	29
Ca^{2+}	lipophilic bistartro-18-crown-6 dicarboxylate	1-hexanol/$CHCl_3$ (10/90), 2.5	3.2×10^{-3}	1×10^{-3}	3.2	8

[a] V_{max}^{rep} is the highest reported rate in a given study; in order to ensure that this rate would correspond more or less closely to an actual V_{max} (i.e., to half-saturated carrier) only studies reporting many comparative experiments were selected; unit: mmol·h^{-1}·cm^{-2}. [b] Unit: mmol·h^{-1}·cm^{-2}·M^{-1}. [c] P^-: picrate anion. [d] Extrapolated to 50% complexed carrier (from reported values of 15, 2, and 22% complexed beauvericin, 4′-methylbenzo-18-crown-6, and (−)-*N*-(1-naphthyl)methyl-α-methylbenzylammonium, respectively). [e] For these values, the literature data correspond to 50% complexed carrier.

rates of transport decrease so rapidly with time that the commonly used selectivity criterion V_A/V_B should be replaced by the more useful one S_{Aout}/S_{Bout}. This ratio has been calculated by resolution of the coupled linear differential equations for the case of two substrates S_A and S_B in exchange diffusion with S_2 ($S_A + S_B$ corresponding to the single substrate S_1 of Figure 6; see Appendix D). The general result which emerges from these simulations is that if $K_{eA} > K_{eB}$, S_{Aout} is always higher than S_{Bout}, whereas V_A becomes smaller than V_B toward the end of a transport run (see also Figure 9 in Appendix D for an extreme case).

Nevertheless, although the rate curves are symmetrical with respect to $K_e = 1$ (Figure 7), the transport selectivity is quite different on each half of the bell. Figure 8 shows the variation of the selectivity as the transport goes on: for $K_{eA}, K_{eB} \ll 1$ (i.e., on the left half of the curves in Figure 7), the selectivity S_{Aout}/S_{Bout} remains almost equal to the thermodynamic extraction selectivity K_{eA}/K_{eB} nearly up to the end of the experiment; in the opposite situation ($K_{eA}, K_{eB} \gg 1$), saturation at the *out* interface soon influences the rates of transport and the selectivity falls down to $S_{Aout} \sim S_{Bout}$. Thus the substrate separation power of a transport experiment is $1 \leq S_{Aout}/S_{Bout} \leq K_{eA}/K_{eB}$ ($K_{eA} > K_{eB}$).

This general result no longer holds if the membrane is made *asymmetric*.[9,10] For instance, when $K_{eA}, K_{eB} \gg 1$, $K_{eA} > K_{eB}$, and the extraction selectivity in favor of S_A is slightly higher at the *out* than at the *in* interface, then $S_{Bout} > S_{Aout}$, i.e., transport selectivity is *reversed* compared to extraction selectivity! Such a situation has been found in the transport of the racemic mandelate anion by a chiral ammonium carrier in exchange diffusion with Cl^-.[19]

The other mechanisms of transport lead to the same conclusions, namely that the selectivity of competitive transport is the highest for extraction equilibrium constants lower than $|K_e|_{max}$. Keeping in mind that the rate of transport is proportional to loading of the carrier at the *in* interface, an *efficient* (fast and selective) system should have K_e of the best extracted substrate about equal to $|K_e|_{max}$; the value of $|K_e|_{max}$ in turn depends on the mechanism and experimental conditions (see previous sections).

Transport Limited by Complexation Kinetics. The equations developed above account well for the carrier-assisted transport of substrates through bulk-liquid membranes in various experimental conditions even at extremely high K_e values. However, this does not necessarily imply that the rate is limited by diffusion at the interfaces, allowing extraction equilibrium to be reached. Indeed assuming rates of interfacial exchange (complex formation and dissociation) or exchange within the membrane[11] to be limiting, or even mixed processes to be of the same order of magnitude,[9,10] leads to roughly the same rate equations where the rate V is proportional to (L_0, $S_{in} - S_{out}$) and which differ only at high saturation of the carrier. Let us consider for instance the process of Figure 1 ($K_e = k_a/k_d$) in the case of a transport controlled by complexation kinetics (complexation and decomplexation rate constants k_a and k_d). At each interface, the forth and back rates are unequal allowing a net entrance $V_{in} = k_a S_{in} L - k_d LS$ at *in* and a net release $V_{out} = k_d LS - k_a S_{out} L$ at *out*. The steady-state condition $V_{in} = V_{out}$ leads to

$$LS/L = \tfrac{1}{2} K_e S_0$$

$$V = k_a \frac{L_0}{2} \frac{S_{in} - S_{out}}{1 + K_e S_0/2} \qquad (10)$$

which resembles (3). Two limiting situations can be envisaged.

If $K_e S_0 \ll 1$, the rate is controlled by complex formation at *in*, the carrier is almost empty, and

$$V \sim k_a (L_0/2)(S_{in} - S_{out})$$

At high substrate concentrations allowing saturation of the carrier ($K_e S_0 \gg 1$), the rate is controlled by the release at *out*, $LS \sim L_0$, and

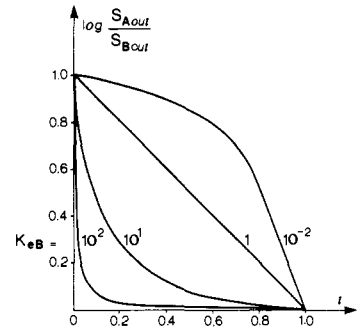

Figure 8. Variation of the transport selectivity, i.e., the ratio of substrate concentrations in the receiving aqueous phase (S_{Aout}/S_{Bout}), as a function of the extent of transport described by $f = (S_{Aout} + S_{Bout})/S_0$ in the case of two substrates S_A and S_B ($S_A + S_B$ corresponding to the single substrate S_1 of Figure 6) in competitive exchange diffusion with a back-transported substrate S_2; initial concentration $S_0 = S_2 = 2S_A = 2S_B$; the curves correspond to different values of the extraction equilibrium constants K_{eB} and $K_{eA} = 10K_{eB}$.

$$V \sim k_d L_0 \frac{S_{in} - S_{out}}{S_0}$$

Thus the *highest rate* ($k_d L_0$) is obtained when *the carrier is entirely loaded with substrate*, in contrast to the diffusion-limited case (see section 1) *and* to experiments[6b,20] which give a rate maximum for a half-loaded carrier.

Another argument in favor of a diffusion-limited rate for transport through bulk-liquid memembranes comes from a survey of the literature data. With use of the highest rate reported V_{max}^{rep} in a given study, as an approximation of V_{max}, V_{max}^{rep}/L_0 should be related either to diffusion characteristics or to complexation kinetics. Table I lists results from transport experiments performed with widely different substrates and carriers; in addition, they correspond to undefined fractions of substrate transported, so that it is not known how close V_{max}^{rep} is to V_{max}. Nevertheless, the V_{max}^{rep}/L_0 values calculated from these data stay within a remarkably narrow range; such a result is compatible with a diffusion-limited transport where $V_{max}/L_0 = D/2l$ (see eq 4) but not with a model of transport limited by complexation–decomplexation rates in homogeneous phase, which vary over many powers of ten.

Furthermore, these values are of the order of $D/2l$ calculated with use of a diffusion coefficient of ca. 10^{-5} cm^2/s^{-1} [17,30] and the thickness of a Nernst layer (50–300 μ),[12b,16] $D/2l \sim 2$–10×10^{-4} cm·s^{-1} (i.e., 0.5–3.5 mmol·h^{-1}·cm^{-2}·M^{-1}; see Table I).

Thus, it seems that transport is limited by diffusion in most if not all bulk systems, although a change toward a reaction-limited process cannot be excluded at high K_e (low k_d), for instance in the transport of transition-metal cations via kinetically very sluggish complexes formed with polyazamacrocyclic carriers.

Conclusion

In the previous sections, a diffusion-limited kinetic treatment has been explicitely applied to carrier-mediated transport processes through thick liquid membranes, covering a wide range of rates and selectivities. The detailed computational results indicate that this assumption is sufficient for explaining and predicting the behavior of these systems and that there is no need to invoke a change in rate-limiting step at high values of the stability and extraction constants. The same treatment may be successfully applied to other types of carrier-mediated transport (transport of divalent cations by neutral or charged ligands, countertransport of proton by weakly acidic carriers, etc.). Despite the need for a computer for solving numerically the mathematical equations involved and for performing the numerical explorations, the main conclusions reached are rather straightforward. *Transport takes place* only when the concentration of substrate is high enough to allow complex formation in the membrane ($S_0 \gtrsim K_e^{-1}$) and goes on as long as carrier saturation at the receiving interface is low ($S_{out} < K_e^{-1}$). The latter restriction may be bypassed in many ways by an irreversible process at the *out* interface, like removing the incoming substrate (flow apparatus, complexation, or precipitation of the substrate), or changing the nature of the carrier (for instance by protonation of a weak acidic carrier). The *transport selectivity* of a given carrier for various substrates is reflected in the concentration (and not rate) ratios determined in true competition experiments; the thermodynamic extraction selectivity may be maintained in time by using the same procedures as above.

It is hoped that the treatment developed here will help clarify the behavior of artificial transport systems and provide guidelines for achieving efficient and selective transport, in a given set of conditions and with defined carrier molecules.

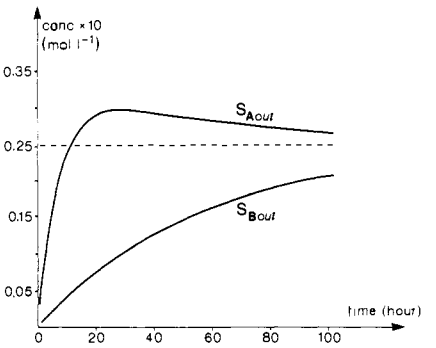

Figure 9. Simulation of a transport experiment consisting of two substrates S_A and S_B (where $S_A + S_B$ corresponds to the single species S_1 of Figure 6) in competitive exchange diffusion with a back-transported species S_2 for the following case: initial concentrations $S_A = S_B = S_2/2 = 5 \times 10^{-2}$ M; $K_{eA} = 1$, $K_{eB} = 0.1$, $V_{max} = 5 \times 10^{-3}$ mol·h^{-1}·cm^{-2}.

Appendix A

Setting $V/V_{max} = y$, all rate equations can be solved as quadratic equations of the form

$$AK_e^2 + BK_e + C = 0 \qquad (11)$$

Development of (7) yields

$$A = S_0 y(1 - f)(S_0 f + 0.5L_0 y)$$

$$B = 0.5L_0 y^2 + (S_0 + 0.5L_0)y - S_0(1 - 2f)$$

$$C = y$$

For a given set (S_0, L_0, f), (11) was repeatedly computed on a PDP 11/44 computer with a 0.01 increment for y until its determinant became negative. Then back to the last real roots, the increment was set to 0.001 and the process repeated. The calculated ($K_e'(y_i)$, $K_e''(y_i)$) roots were arranged in increasing order and $y = g(K_e)$ was plotted on a Versatec line printer with interpolation between the calculated points, yielding the smooth curves shown in Figure 3. Taking into account the concentration gradient at the aqueous *in* interface ($S_{i,in} = S_{in} - 0.5\ L_0 y$) introduces additional terms in A and B which may be neglected if $S_0 \gg L_0$ and $f \ll 0.5$. At the maximum of the bell-shaped curve, the roots of (11) are equal; thus $|K_e|_{max}^2 = C/A$ which for $f \to 0$ reduces to $2/(S_0\ L_0 y_{max})$.

Appendix B

With the conditions in eq 5 and eq 6, eq 8 can be rearranged as eq 11, with

$$A = S_0^2 y(0.25L_0^2 y^2 + S_0 L_0 f y + S_0^2 f^2)$$

$$B = 0.25\ L_0^2 y^3 + L_0(S_0 f + 0.25L_0)y^2 + S_0(S_0 + L_0 f + S_0 f^2)y - S_0^2(1 - f^2)$$

$$C = y$$

(20) Pinkerton, M.; Steinrauf, L. K.; Dawkins, P. *Biochem. Biophys. Res. Commun.* **1969**, *35*, 512–518.
(21) Roeske, R. W.; Isaac, S.; King, T. E.; Steinrauf, L. K. *Biochem. Biophys. Res. Commun.* **1974**, *57*, 554–561.
(22) Kobuke, Y.; Hanji, K.; Horiguchi, K.; Asada, M.; Nakayama, Y.; Furukawa, J. *J. Am. Chem. Soc.* **1976**, *98*, 7414–7419.
(23) Ramdani, A.; Tarrago, G. *Tetrahedron* **1981**, *37*, 991–1000.
(24) Fyles, T. M.; Malik-Diemer, V. A.; Whitfield, D. M. *Can. J. Chem.* **1981**, *59*, 1734–1744.
(25) Maruyama, K.; Tsukube, H.; Areko, T. *J. Am. Chem. Soc.* **1982**, *104*, 5197–5203.
(26) Shinkai, S.; Kinda, H.; Araragi, Y.; Manabe, O. *Bull. Chem. Soc. Jpn.* **1983**, *56*, 559–563.
(27) Izatt, R. M.; Lamb, J. D.; Hawkins, R. T.; Brown, P. R.; Izatt, S. R.; Christensen, J. J. *J. Am. Chem. Soc.* **1983**, *105*, 1782–1785.
(28) Izatt, R. M.; Dearden, D. V.; Brown, P. R.; Bradshaw, J. S.; Lamb, J. D.; Chistensen, J. J. *J. Am. Chem. Soc.* **1983**, *105*, 1785–1790.
(29) Lamb, J. D.; Brown, P. R.; Christensen, J. J.; Bradshaw, J. S.; Garrick, D. G.; Izatt, R. M. *J. Membr. Sci.* **1983**, *13*, 89–100.
(30) Reid, R. C.; Prausnitz, J. M.; Sherwood, T. K. "The Properties of Gases and Liquids", MacGraw-Hill: New York, 1977.

and solved as described previously. $|K_e|_{max} = (C/A)^{1/2}$ contains a sum of terms of the same order of magnitude; for $f \rightarrow 0$, $|K_e|_{max} \rightarrow 2/(S_0L_0y_{max})$.

Appendix C

Here the quadratic eq 11 becomes

$$A = -0.25L_0^2y^3 + 0.5S_0L_0(1 - 2f)y^2 + S_0^2f(1 - f)y$$

$$B = 0.5L_0^2y^3 - S_0L_0(1 - 2f)y^2 + S_0(S_0f^2 + S_0(1 - f)^2 + L_0)y - S_0^2(1 - 2f)$$

$$C = A$$

The maximum rate was calculated from (11) with $K_e = 1$

$$y_{max} = (1 - 2f)/(1 + L_0/S_0)$$

Appendix D

For two substrates S_A and S_B in competitive exchange diffusion with S_2, eq 9 becomes

$$\frac{dS_{Aout}}{dt} = V_{max}K_{eA}\frac{N}{D_1D_2}$$

$$N = S_{Ain}S_{in} - S_{Aout}S_{out} + K_{eB}(S_{Ain}S_{Bout} - S_{Aout}S_{Bin})$$

$$D_1 = (K_{eA}S_{Ain} + K_{eB}S_{Bin} + S_{Aout} + S_{Bout})$$

$$D_2 = (K_{eA}S_{Aout} + K_{eB}S_{Bout} + S_{Ain} + S_{Bin})$$

with

$$S_{A(B)in} = S_0 - S_{A(B)out}$$

$$S_{in(out)} = S_{Ain(out)} = + S_{Bin(out)}$$

A similar equation holds for dS_{Bout}/dt, where subscripts A are exchanged for B and conversely. The coupled linear differential equations were solved numerically for a given set (S_0, V_{max}, K_{eA}, K_{eB}) with initial conditions $S_{A(B)in} = 0.5S_{2out} = S_0$. The concentrations $S_{A(B)out}$ were plotted against time (Figure 9) and the selectivity S_{Aout}/S_{Bout} against f (Figure 8).

Micellar Systems as Devices for Enhancing the Lifetimes and Concentrations of Free Radicals[1]

T. J. Burkey and D. Griller*

Contribution from the Division of Chemistry, National Research Council of Canada, Ottawa, Ontario, Canada K1A 0R6. *Received June 11, 1984*

Abstract: Optical modulation spectroscopy was used to monitor the second-order decay kinetics of phenylthiyl (I) and mesitythiyl radicals (II) in both heptane and sodium dodecyl sulfate (SDS) solutions. The self-reactions of the thiyl radicals were found to be diffusion controlled in the hydrocarbon solvent. Little change was observed in the decay kinetics of I when the solvent was aqueous SDS (0.2 M), suggesting that the radical was not strongly partitioned into the micelles. However, enhancements of a factor of ca. 50 in both the lifetime and concentration of II were observed in 0.05 M SDS, implying that the larger radical was effectively caged within the micelles. Kinetic analysis led to a value of 2×10^3 s^{-1} for the exit rate constant of II from SDS micelles.

The behavior of radical pairs formed photochemically in micelles has been the focus of extensive investigation.[2-14] Often the micelle functions as a temporary cage for the radical pair, in which case, radical-radical encounters are frequent and reaction is only restricted if the radical pair is in the triplet state.[2] Even with this restriction, intersystem crossing to the singlet state and subsequent reaction normally occurs in the submicrosecond time scale.[6,7] Of course, micelles are not perfect jailors and escape by one of the radicals is an important process which forms the subject of this paper.

Once free of its partner, a given radical has two major pathways for decay. If there is no strong preference for the micellar environment, then the concentration of radicals in the aqueous phase will be relatively high so that radical-radical reaction in that phase will be the most important mode of decay. The decay kinetics will be second order and will hardly be perturbed by the presence of the micelles.

For a radical which shows a strong preference for the micellar environment, the radical concentration in the aqueous phase will be low. Decay will then occur by a mechanism in which the radical visits a number of micelles by repeated exit and entry until it finds one which contains another radical, when reaction will generally occur. In this instance decay may again follow second-order kinetics (vide infra) with the exit process being the rate-controlling step.

It is this second case which is intruiging, since it suggests the possibility that the rate constant for exit from the micelle can be measured by following the overall rate of radical decay. Moreover,

(1) Issued as NRCC publication 23904.
(2) Turro, N. J.; Kraeutler, B.; Anderson, D. R. *J. Am. Chem. Soc.* **1979**, *101*, 7435.
(3) Turro, N. J.; Kraeutler, B. *Acc. Chem. Res.* **1980**, *13*, 369.
(4) Turro, N. J.; Chow, M.-F.; Chung, C.-J.; Weed, G. C.; Kraeutler, B. *J. Am. Chem. Soc.* **1980**, *102*, 4843.
(5) Lehr, G. F.; Turro, N. J. *Tetrahedron* **1981**, *37*, 3411.
(6) Scaiano, J. C.; Abuin, E. B. *Chem. Phys. Lett.* **1981**, *81*, 209.
(7) Turro, N. J.; Chow, M.-F.; Chung, C.-J.; Tanimoto, Y.; Weed, G. C. *J. Am. Chem. Soc.* **1981**, *103*, 4574.
(8) Equation 5 is based upon the assumption that reaction 3 proceeds with 100% efficiency. However, this assumption is not quantitatively correct since some escape from the micelle is likely to occur before radical-radical reaction takes place. Comparison with data for the micellar escape of triplet radical pairs[6] suggests that reaction 3 will proceed with an efficiency of ca. 70%. No correction was introduced to account for this effect since it is small with respect to the other experimental errors involved in this work.
(9) Turro, N. J.; Chow, M.-F.; Chung, C.-J.; Kraeutler, B. *J. Am. Chem. Soc.* **1981**, *103*, 3886. Turro, N. J.; Anderson, D. R.; Chow, M.-F.; Chung, C.-J.; Kraeutler, B. *J. Am. Chem. Soc.* **1981**, *103*, 3892.
(10) Turro, N. J.; Mattay, J. *J. Am. Chem. Soc.* **1981**, *103*, 4200.
(11) Scaiano, J. C.; Abuin, E. B.; Stewart, L. C. *J. Am. Chem. Soc.* **1982**, *104*, 5673.
(12) Turro, N. J.; Weed, G. C. *J. Am. Chem. Soc.* **1983**, *105*, 1861.
(13) Baretz, B. H.; Turro, N. J. *J. Am. Chem. Soc.* **1983**, *105*, 1309.
(14) Thurnauer, M. C.; Meisel, D. *J. Am. Chem. Soc.* **1983**, *105*, 3729.

0002-7863/85/1507-0246$01.50/0 Published 1985 by the American Chemical Society